Polymer Chemistry

Accepted Manuscript

ROYAL SOCIETY OF CHEMISTRY

www.rsc.org/polymers

Journal Name

ARTICLE

Multi-stimuli Responsive Supramolecular Hydrogel Based on Fe^{3+} and Diblock Copolymer Micelles Complexation

Received 00th January 20xx,
Accepted 00th January 20xx

DOI: 10.1039/x0xx00000x

www.rsc.org/

Zhen Tao, Kang Peng, Yujiao Fan, Yunfei Liu and Haiyang Yang*

The stimuli-triggered degradable hydrogels have found broad applications in controlled release of drugs, fragrances, flavourings and fertilizers. Recently, multi-stimuli responsive micelle-based hydrogels has become focus, since they could respond to a combination of external stimulus. Herein, a multi-stimuli responsive supramolecular hydrogel with great potential to biomedical application was prepared, which composed of the micelle-forming diblock copolymer poly[(N-isopropylacrylamide-*co*-2-nitrobenzyl acrylate)-*block*-(N,N-dimethylacrylamide-*co*-acrylic acid)] (P(NIPAM-*co*-NBA)-*b*-P(DMA-*co*-AA)), and physically cross-linked by supramolecular complexation between AA groups and ferric ions (Fe^{3+}), exhibiting gel-sol transition by UV irradiation, multidentate ligands (EDTA) and redox agent ($Na_2S_2O_4$).

Introduction

Hydrogels are a class of materials formed by three-dimensional cross-linked hydrophilic network[1, 2], which are able to trap molecules with various physiochemical properties[1, 3, 4] and controlled release the guest molecules through their network structure by swelling, diffusion and degradation[3, 5-7]. Over the past few decades, extensive attention has paid to the hydrogels for controlled release of drugs, fragrances, flavourings and fertilizers[8-15].

Recently, hydrogels[16-19] constructed from synthetic polymers[20-25] or low-molecular-weight gelators (LMWGs)[26] have been extensively studied. Tong et al.[27] reported a supramolecular hydrogel rely on the complexation of ferric ions (Fe^{3+}) and poly(acrylic acid) (PAA) with dual responses to redox and light, which was promising as devices for encapsulation and localization of bioactive molecules and cells. Zhang et al.[28] developed a photodegradable hydrogel that allow 3D encapsulation of cells, formed by the self-assembly of short peptides with a phototrigger.

Among the strategies of fabrication, hydrogels composed of polymeric nanoparticles, dendrimers and micelles were widely developed to overcome the limitation to associate the hydrophobic molecules[29, 30]. Additionally, the polymer micelle based hydrogels exhibiting a sol-gel transitions are expected to be applied in cancer medicine[14, 31], tissue engineering[32, 33] and controlled 3D cell culture[34]. Duvall et al.[35] prepared a triblock polymer micelle-based thermoresponsive hydrogel formed *in situ* at physiologic temperature, incorporating reactive oxygen species (ROS) triggered degradation and drug release.

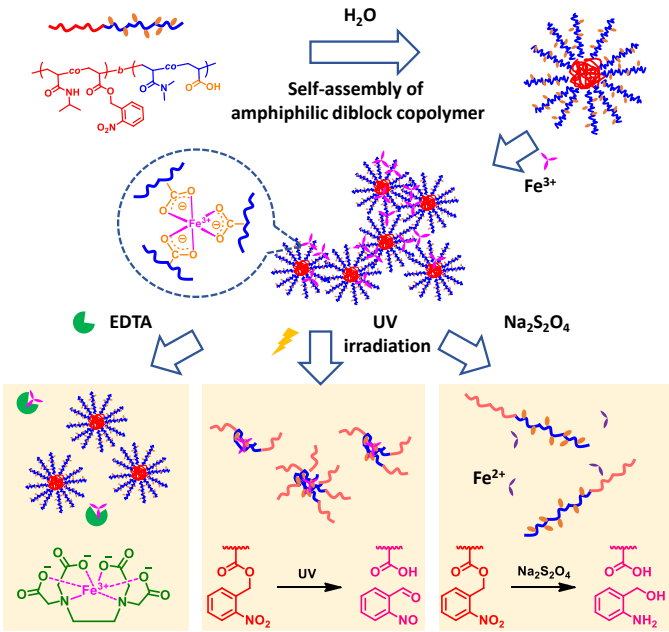

Scheme 1. *Schematic representation of gelation by micelles and complexation of Fe^{3+} and polymer chains, and gel-sol transition triggered by EDTA, UV irradiation and $Na_2S_2O_4$.*

The stimuli-responsive hydrogels could adapt to the external stimuli, playing a significant part in diverse applications from biomedicine to electromechanical systems[17]. Notably, there has been increasing interest in the development and applications of dual and multi-responsive degradable hydrogels, since their enriched versatility leaded by a combination of two or more external stimulus (occur simultaneous or in a sequential manner) [36]. For example, Nitschke[4] et al. have

a. CAS Key Laboratory of Soft Matter Chemistry, School of Chemistry and Materials Science, University of Science and Technology of China, Hefei, 230026, P. R . China.

† Footnotes relating to the title and/or authors should appear here.
Electronic Supplementary Information (ESI) available: [details of any supplementary information available should be included here]. See DOI: 10.1039/x0xx00000x

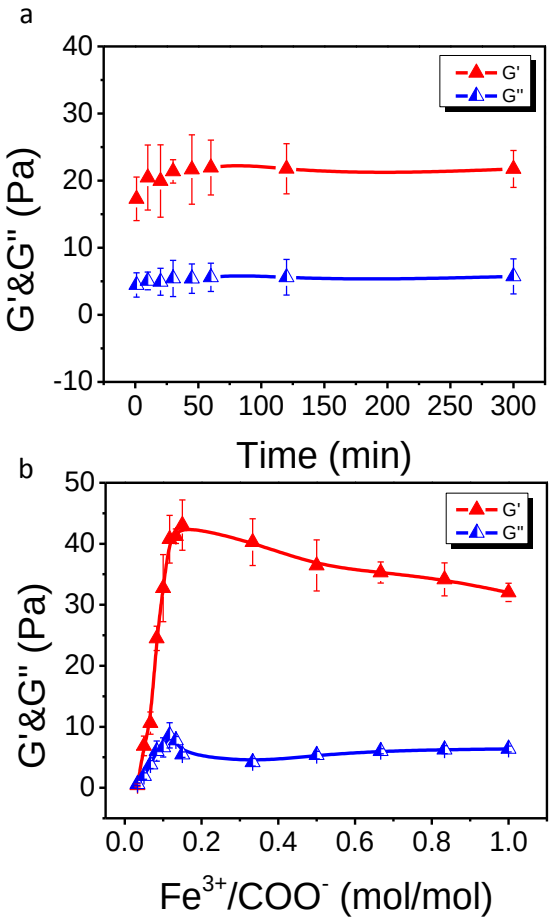

Figure 1. *G' and G" versus Fe^{3+}/COO^{-} of P1 hydrogel.*

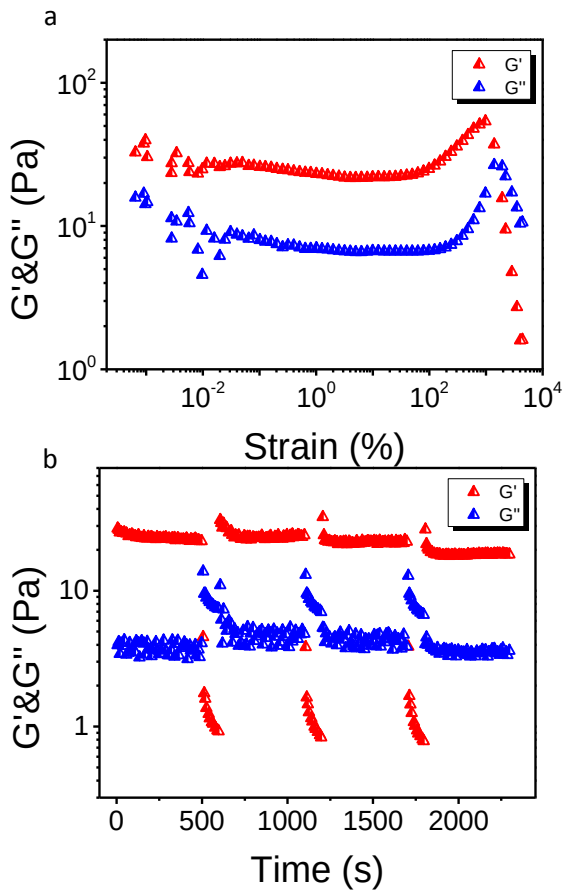

Figure 2. *G' and G" versus (a) frequencies and (b) times curves of P1 hydrogel.*

developed a metal-organic cage-cross-linked polymeric hydrogel, presenting responses to acid, amine and aldehyde, which allows selective encapsulation and graded release of cargo.

Herein, we report a hydrogel crosslinked by complexation between Fe^{3+} and micelles, which were assembled by amphiphilic diblock copolymer poly[(N-isopropylacrylamide-*co*-2-nitrobenzyl acrylate)-*block*-(N,N-dimethylacrylamide-*co*-acrylic acid)] (P(NIPAM-*co*-NBA)-*b*-P(DMA-*co*-AA)), with degradation mechanism triggered by multiple stimuli, as shown in Scheme 1.

The incorporated hydrophobic NBA groups, resulting in a lower low critical solution temperature (LCST) of the random P(NIPAM-*co*-NBA) block (with 6 mol % of NBA, LCST = 6 °C), would convert into hydrophilic AA groups upon UV irradiation, leading to gel-sol transition due to an increasing of LCST to 55 C..[37, 38]

Meanwhile, the complexation between AA groups and Fe^{3+} would disassemble by addition of competing multidentate ligands (for example, EDTA). On removal of Fe^{3+}, the hydrogel would disperse into solution, as a result of the absence of crosslinking.

Further, the nitro groups of NBA moieties would be reduced to amino groups when reacting with reducing agent (for example, $Na_2S_2O_4$), followed by a 1,4-rearrengenment-elimination.[39-41] At the same time, Fe^{3+} would be reduced to ferrous ions (Fe^{2+}) by $Na_2S_2O_4$, leading to a much weaker complexation between AA groups[42, 43]. Thus, the hydrophobic cores of micelles and the complexation between Fe^{3+} and AA groups would be disrupted simultaneously, in the presence of $Na_2S_2O_4$.

The hydrogel could response to light, multidentate ligands and reducing agent simultaneously or in a sequential manner, which could be beneficial for selective encapsulation and sequential release of guest molecules.

Experimental

Materials

N-isopropylacrylamide (NIPAM, 97%, Aldrich) was recrystallized twice from a mixture of n-hexane and benzene (v/v = 2:1) prior to use. 2-Nitrobenzyl acrylate (NBA)[37, 38] and 4-cyanopentanoic acid dithiobenzoate (CTA) were prepared according to the literature.[44] 2,2'-Azobis(2-methylpropionitrile) (AIBN, 99%, Aldrich) was recrystallized from 95% ethanol and stored at -20 °C. N,N-dimethylacrylamide (DMA, 99%, Aldrich) and 1,1,3,3-Tetramethylguanidine (TMG, 98%, Aldrich) were distilled under reduced pressure. Acrylic acid (AA, 98%, Sinopharm Chemical Reagent Co. Ltd.) was distilled under reduced pressure and stored at -20 °C. Benzyl chloride (Sinopharm Chemical Reagent

Co. Ltd.), ferric chloride hexahydrate ($FeCl_3 \cdot 6H_2O$, Sinopharm Chemical Reagent Co. Ltd.), sodium dithionite ($Na_2S_2O_4$, 90%, Aladdin) and ethylenediaminetetraacetic acid (EDTA, Sinopharm Chemical Reagent Co. Ltd.) were used as received. The murine 4T1 murine mammary carcinoma cells were purchased from the Shanghai Institute of Cell Biology (Shanghai, China). Fetal bovine serum (FBS), trypsin, phosphate

buffered saline (PBS), and Dulbecco's modified Eagle's medium (DMEM) were purchased from GIBCO and used as received. Cell culture lysis buffer, 4',4',6-diamidino-2-phenylindole

(DAPI), 3-(4,5-dimethylthiazol-2,5-diphenyltetrazolium bromide (MTT), propidium iodide (PI, 94%), fluorescein diacetate (FDA), and hematoxylin and eosin (H&E) staining kit were purchased from Beyotime Institute of Biotechnology (Shanghai, China).

Synthetic and Characterization of Polymer

P(NIPAM-*co*-NBA)-macro CTA was synthesized by reversible addition-fragmentation chain transfer (RAFT) polymerization of NIPAM and NBA with AIBN as initiator . Typically, the mixed solution of CTA (42.5 mg, 0.15 mmol), NIPAM (1.12 g, 9.92 mmol), NBA (82 mg, 0.40 mmol), AIBN (5.0 mg, 0.03 mmol) and THF (1.3 mL) was degassed *via* three freeze-pump-thaw cycles and then backfilled with nitrogen. The polymerization was performed at 85 °C for 14 h. The final polymerization mixture was precipitated into an excess of diethyl ether for three times, and dried in a vacuum oven overnight at room temperature, yielding a solid powder (370 mg, yield ~ 30%). The conversion of NIPAM and NBA was determined to be ~ 48% and ~ 76%, respectively based on ^{1}H NMR analysis and the chemical structure of the product was determined to be P(NIPAM$_{0.94}$-*co*-NBA$_{0.06}$)$_{33}$-macro CTA, which is shortened as P(NIPAM-*co*-NBA) in the subsequent section. The macro-CTA with different degree of polymerization (DP) was prepared in a similar way.

P(NIPAM-*co*-NBA)-macro CTA was employed to synthesis the second block of poly(DMA-*co*-AA). Typically, the mixed solution of P(NIPAM-*co*-NBA) (500 mg, 0.13 mmol), DMA (4.06 g, 41.5 mmol), AA (746 mg, 9.3 mmol), AIBN (4.25 mg, 0.03 mmol) and dioxane (10.4 mL) was degassed via three freeze-pump-thaw cycles and then backfilled with nitrogen. After stirring at 80 °C for 4 h, the polymerization was quenched into liquid nitrogen. The resultant amphiphilic diblock copolymer was precipitated into an excess of diethyl ether, and the sediments dissolved in DMSO and precipitated twice into diethyl ether. The final product was dried in a vacuum oven overnight at room temperature, yielding a solid powder (370 mg, yield ~ 40%).

To determine the conversion of AA and the chemical structure of diblock copolymer P(NIPAM-*co*-NBA)-*b*-P(DMA-*co*-AA), a facile and high efficient esterification[45] (yield ~ 100%) was carried out to convert AA into Benzyl acrylate (BA). The conversion of DMA and AA was determined to be ~ 34% and ~ 90%, respectively based on ^{1}H NMR analysis and the chemical structure of the product was determined to be P(NIPAM$_{0.94}$-*co*-NBA$_{0.06}$)$_{33}$-*b*-P(DMA$_{0.6}$-*co*-AA$_{0.4}$)$_{180}$ (P1). The diblock copolymers, P(NIPAM$_{0.94}$-*co*-NBA$_{0.06}$)$_{69}$-*b*-P(DMA$_{0.6}$-*co*-AA$_{0.4}$)$_{180}$ (P2) and P(NIPAM$_{0.94}$-*co*-NBA$_{0.06}$)$_{108}$-*b*-P(DMA$_{0.6}$-*co*-AA$_{0.4}$)$_{180}$ (P3) were synthesized using a similar route.

^{1}H NMR spectra of polymers were recorded in $CDCl_3$ with an AC400 Bruker spectrometer operating at 400 MH.

Preparation and characterization of micelles

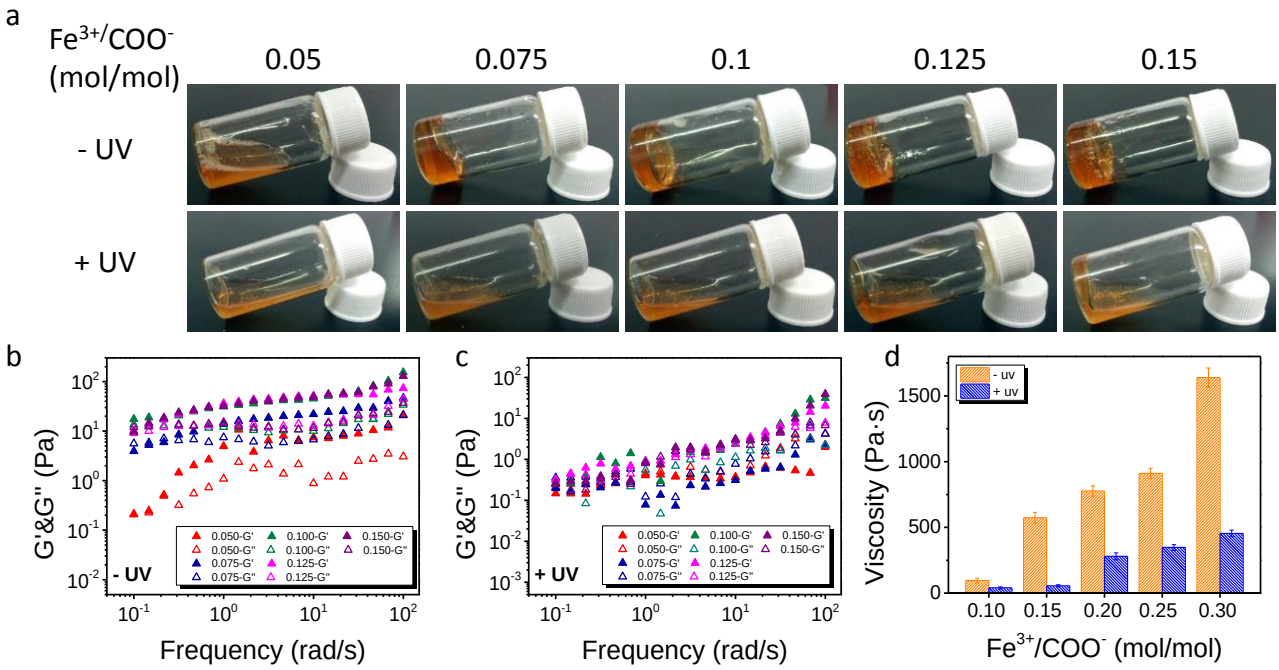

Figure 3. *The gel-sol transition of P1 hydrogel with different Fe^{3+}/COO^-. The photography (a), G' and G" versus frequencies before (b) and after (c) UV irradiation, and viscosity versus times curves Fe^{3+}/COO^- (d).*

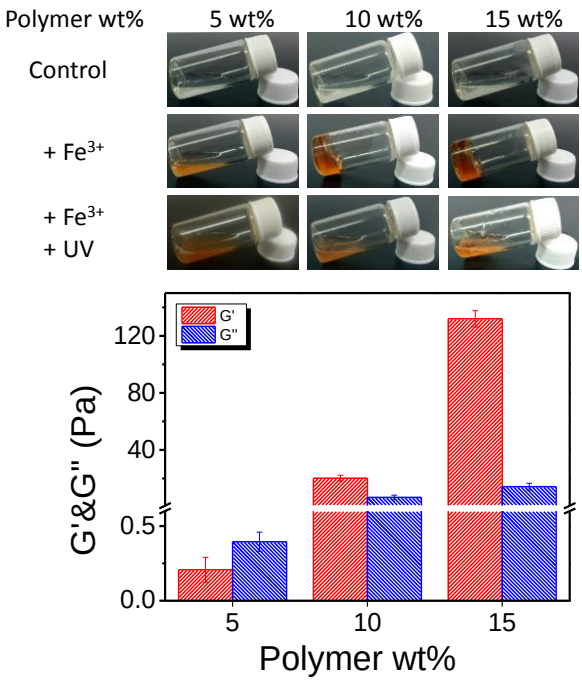

Figure 4. *Photography of the reversed vial test and degradation by UV irradiation of P1 hydrogel at different polymer wt%. (a)G' and G" versus polymer weight percentage of P1 hydrogel.*

The micelles assembled by amphiphilic diblock copolymer directly dissolved into deionized water (DI water) at different polymer weight percentage (5 wt%, 10 wt% and 15 wt%). The size of micelles were characterized by dynamic laser light scattering (DLS) measurements. The critical micelle concentration (CMC) and the stability of micelles were characterized by DLS.

A commercial spectrometer (ALV/DLS/SLS-5022F) equipped with a multi-tau digital time correlator (ALV5000) and a cylindrical 22 mW UNIPHASE He–Ne laser (λ_0 = 632 nm) as the light source was used. Scattered light was collected at a fixed angle of 90° for duration of ~5 min. Distribution averages and particle size distributions were computed using cumulants analysis and CONTIN routines. All data were averaged over three successive measurements. The critical micelle concentration (CMC) and the copolymer micelle stability were also confirmed by concentration- and time-dependent DLS measurements.

Preparation of Hydrogels

Addition of different amount of Fe^{3+} (molar ratio of Fe^{3+}/COO^- = 0.03-1.0) into the micelle solution and vigorous shaking for a few seconds, to compare the influence of parameters on gelation. The reversed vial test method was utilized with varying time intervals from 1min to 300 min, to demonstrate the hydrogel formation and stabilization at room temperature.

To see the UV-triggered degradation of hydrogel, the hydrogel (polymer weight percentage equals to 10 wt%; molar ratio of Fe^{3+}/COO^- = 0.075) was irradiated for 1h by a handheld ultraviolet lamp. To study the EDTA-triggered degradation of hydrogel, the hydrogel was reacted with 50 µL EDTA aqueous solution (molar ratio of EDTA/Fe^{3+} = 1) for 5 min. To investigate the redox-triggered degradation of hydrogel, the hydrogel was incubated with 50µL $Na_2S_2O_4$ aqueous solution (molar ratio of $Na_2S_2O_4$/NBA = 1) for 20 min.

Rheology of Hydrogels

Rheological measurements were conducted on a TA AR-G2 rheometer using a cone-plate of 40 mm diameter with a cone angle of 1°. The frequency-sweep spectra were recorded in a constant-strain (0.04 %) mode over the frequency range of 0.1-100 rad/s at 25 °C. The strain-sweep spectra were recorded in a constant frequency of 6.28 rad/s over the strain range of 0.001-4000 % at 25 °C.

To investigate the recovery properties of the samples in response to applied shear forces, the samples were placed between the cone-plate and the platform with special care. We used the following programmed procedure (applied shear force, expressed in terms of strain; duration in parentheses): 1 % (500 s) / 4000 % (100 s) / 1 % (500 s) / 4000 % (100 s) / 1 % (500 s) / 4000 % (100 s) / 1 % (500 s).

The viscosity of samples was determined from the linear region during the frequency sweep.

In vitro cytotoxicity evaluation before complexation.

4T1 cells were seeded onto 96-well plates at a density of 1×104 cells/well in 100 µL DMEM with 10% FBS at 37 °C with 5% CO_2 humidified atmosphere. After 24 h incubation, the DMEM medium was replaced with fresh culture medium, and the cells were treated with P1 micelle solution at 10 wt%. After 12 h incubation, the medium in each well was replaced with fresh cell culture medium for another 48 h incubation. MTT solution (20 μL, 5 mg/mL in PBS buffer) was added to each well and incubated 4 h for reaction. The medium in each well was then removed and 200 μL of DMSO was added to dissolve the internalized purple formazan crystals. The plate was subjected to gently agitation for 30 min until all the crystals were dissolved. The absorbance at wavelength of 480 nm was recorded by a microplate reader (Thermo Fisher).

In vitro cytotoxicity evaluation after complexation/degradation

4T1 cells were seeded onto 96-well plates at a density of 1×104 cells/well in 100 µL DMEM with 10% FBS at 37 °C with 5% CO2 humidified atmosphere. After 24 h incubation, the DMEM medium was replaced with fresh culture medium, and the cells were treated with P1 micelluar solution at 10 wt%. Addition of Fe^{3+} (Fe^{3+} : COO^- = 0.075) into the copolymer micelle solution to allow the hydrogels to fully solidify. After 12 h hydrogel incubation, the respective plates were irradiated by UV, or added EDTA or $Na_2S_2O_4$ solution at appropriate concentration to de-solidify the hydrogel. Then the medium in each well was replaced with fresh cell culture medium for another 48 h incubation. MTT solution (20 μL, 5 mg/mL in PBS buffer) was added to each well and incubated 4 h for reaction. The medium in each well was then removed and 200 μL of DMSO was added to dissolve the internalized purple formazan crystals. The plate was subjected to gently agitation for 30 min until all the crystals

Table 1. *The physicochemical properties of the hydrogels. The gelation of the hydrogel was visually recognized by the reversed vial test method. The storage moduli (G') and the loss moduli (G") of the hydrogels were carried out on a rotated rheometer.*

Entry	Polymer	Polymer wt%	Fe^{3+}/COO^-	-UV		+UV	
				G'(Pa)	G"(Pa)	G'(Pa)	G"(Pa)
P3	$P(DMA_{0.6}\text{-co-}AA_{0.4})_{180}\text{-}b\text{-}P(NIPAM_{0.94}\text{-co-}NBA_{0.06})_{109}$	15	0.4	59.8	14.8	29.2	35.9
P2	$P(DMA_{0.6}\text{-co-}AA_{0.4})_{180}\text{-}b\text{-}P(NIPAM_{0.94}\text{-co-}NBA_{0.06})_{69}$	15	0.075	72.4	28.5	15.6	18.8
P2	$P(DMA_{0.6}\text{-co-}AA_{0.4})_{180}\text{-}b\text{-}P(NIPAM_{0.94}\text{-co-}NBA_{0.06})_{69}$	10	0.15	46.6	22.4	2.3	3.3
P1	$P(DMA_{0.6}\text{-co-}AA_{0.4})_{180}\text{-}b\text{-}P(NIPAM_{0.94}\text{-co-}NBA_{0.06})_{33}$	10	0.075	20.2	6.6	0.13	0.26

were dissolved. The absorbance at wavelength of 480 nm was recorded by a microplate reader (Thermo Fisher).

Results and discussion

Synthesis and characterization of polymer

The diblock copolymer P(NIPAM-*co*-NBA)-b-P(DMA-*co*-AA) was prepared by sequential reversible addition-fragmentation chain transfer (RAFT) polymerization(Figure S1), and characterized by ^{1}H NMR analysis (Figure S2), combining the post-modification reaction (Figure S3). The first step involves the synthesis of P(NIPAM-*co*-NBA) block. The NBA molar fractions was calculated to be 6 %, with degree of polymerization (DP) being 33 (P1), 69 (P2) and 109 (P3), respectively, from the ratio of the characteristics of NIPAM moiety at 4.0 ppm, the characteristics of NBA moiety at 5.5 ppm and the characteristics of CTA moiety in ^{1}H NMR spectra. Then the P(NIPAM-*co*-NBA)-macro CTA was employed for RAFT polymerization of DMA and AA. The appearance of the CH_3 proton peak at 2.8-3.0 ppm of DMA moiety from the ^{1}H NMR spectra confirmed the successful polymerization. The molar fractions of AA was further determined by post-modification reaction, a high effective esterification (yield ~ 100%), which converted the P(DMA-*co*-AA) into P(DMA-*co*-BA). Based on the appearance of CH proton peak at 5.0 ppm, the characteristics of BA moiety, the AA molar fraction was calculated to be 40%, with DP of P(DMA-co-AA) being 180.

Preparation and characterization of micelles

As showed in Table S1, dynamic light scattering (DLS) measurement revealed intensity-average hydrodynamic diameter, $\langle D_h \rangle$, and polydispersity (PDI) for each sample. The CMC value was confirmed to be 0.17 mg/mL by concentration-dependent DLS measurements (Figure S4a). The time-dependent DLS measurements suggested the good stability of copolymer micelles (P1) over 1 week duration (Figure S4b).

Preparation and rheological characterization of hydrogels

On addition of Fe^{3+} into the polymer solution, a transparent brown coloured hydrogel was created with a few seconds, due to the fast complexation of Fe^{3+} and the carboxyl groups.[27, 46] To investigate the gelation and hydrogel stabilization, rheological measurements were conducted with varying time intervals or different Fe^{3+}/COO^- molar ratios (Figure 1).

From the curves of the storage moduli (G')and the loss moduli (G") versus time as shown in Figure 1a, G' substantially exceeded G" for all configurations, implying the hydrogels were obtained since 1 min after addition of Fe^{3+}.[47, 48] Moreover, the nearly time-independence of the G' and G" values after 10 min was an indication of the hydrogel stabilization crosslinked by complexation between Fe^{3+} and AA groups established in 10 min. The rapid gelation and hydrogel stabilization procedure were owing to the fast binding of Fe^{3+} to AA groups. Thereby, all the rheological measurements were conducted after 10 min of preparation of the hydrogel.

From the curves of the G' and G" versus Fe^{3+}/COO^- molar ratios as shown in Figure 1b, it could be observed that the hydrogels were formed at a molar ratio of Fe^{3+}/COO^- above 0.05.

Increasing the molar ratio from 0.05 to 0.12, both of G' and G" increased considerably, with obvious molar ratio dependence. When the molar ratio increased over 0.15, both of the values of G' and G" decreased gently, which might be attributed to the gradually increasing ionic strength.

According to the literature, the hydrogel based on the coordination of Fe^{3+} and carboxyl groups was expected to be self-healable, because of the dynamic binding.[49, 50] To figure out the linear viscoelastic regime and the gel-sol transform point of the as-prepared hydrogel firstly, the strain sweep tests were conducted from 0.01 % to 4000 % strain at 25 °C, with a constant frequency of 6.28 rad/s. As shown in Figure 2a, the values of G' and G" remain constant over strain ranging from 0.1 % to 100 %, suggesting no apparent damage forming in the hydrogel. When the strain increased over 1000%, the hydrogel reversed

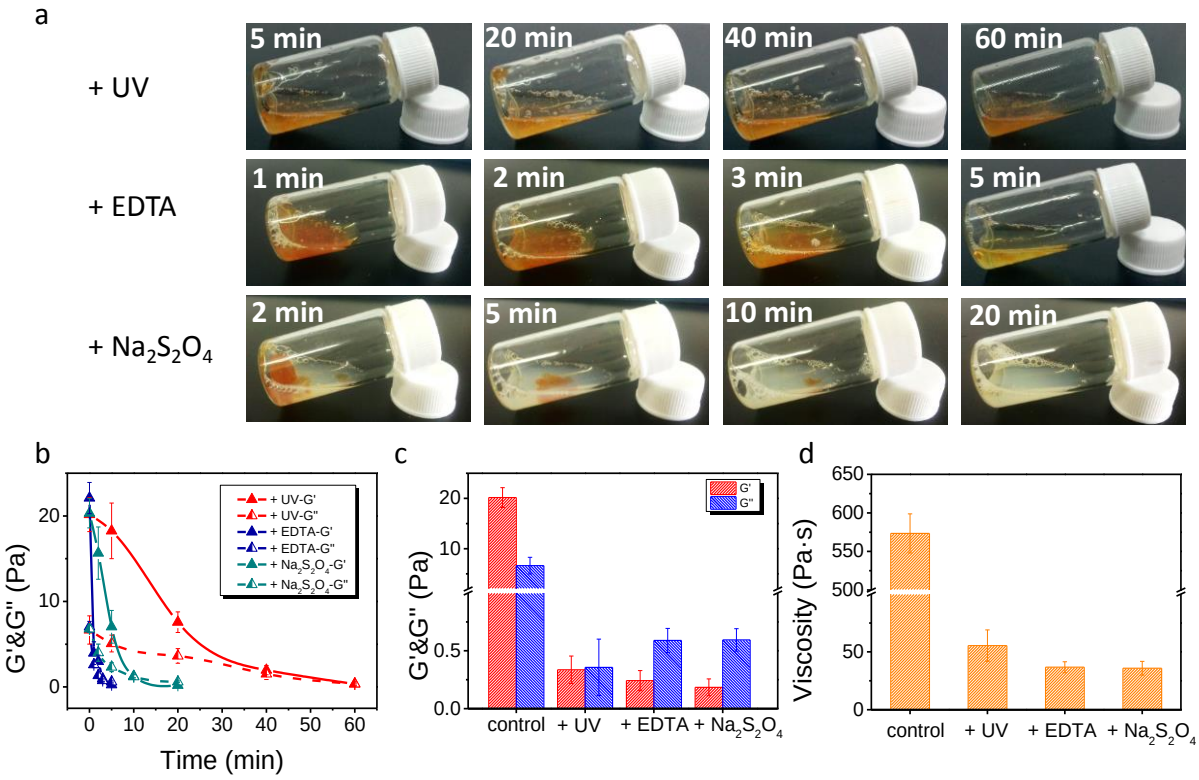

Figure 5. *The photography of the gel–sol transitions (a), the G' and G" versus time (b), and G' and G" (c), and viscosity (d) of P1 hydrogels triggered by multiple stimuli.*

into a liquid state since the dislocation or cut-off of physical cross-linking points, as is evident from the sharp decrease of values of G' and G" with a crossing over of G' and G" at higher strain.

Then, the self-healing property of the hydrogel was examined by pulse deformation program.[51, 52] As shown in Figure 3b, when strain decreased from 4000 % back to 1 %, the recovery of G' and G" values to their initial states, demonstrated the self-healing capability of this hydrogel, which resulted from the rapid autonomous reconstruction of the network. Further, the G' and G" values were almost constant over cyclic tests and the recovery rate was relatively fast.

Degradation of hydrogel upon UV irradiation

The LCST of the copolymer would increase upon UV irradiation, due to the conversion of P(NIPAM-*co*-NBA) into P(NIPAM-*co*-AA), which would lead to the degradation of micelles assembled by diblock copolymer and sol-gel transition. To determine the degradation of the hydrogel triggered by UV irradiation, rheological measures were conducted on hydrogels with different Fe^{3+}/COO^- molar ratios, before and after UV irradiation for 1 h. As shown in Figure 3, a marked frequency dependence of viscoelastic gel properties was observed in frequency-sweep tests for all hydrogel samples, which is typically for hydrogel crosslinked by noncovalent bonds.[53] The increase of the G' and G" at higher frequencies was owing to the relaxation of physical cross-linking points. It was revealed that the G' and G'' values increased with Fe^{3+}/COO^- molar ratios ranging 0.05 to 0.125, in agreements with previous characterization (Figure 3d). Upon UV irradiation, both of the G' and G" values decreased dramatically (~ 90 %) and the hydrogel with Fe^{3+}/COO^- molar ratio more than 0.1 would not exhibit the gel-sol transition, on account of higher density of crosslinking points *via* Fe^{3+} and AA groups. Whether the hydrogel underwent the gel-sol transition or not, the viscosity decreased sharply (more than 70 %) after UV irradiation, which is attributed to the disruption of hydrophobic core of micelles.

Under the same condition, rheological measures were undertaken to clarify the effect of polymer weight percentage on the gelation and degradation progress at a fixed Fe^{3+}/COO^- molar ratio of 0.075. It was provided that the G' and G" values were also correlated with the polymer weight percentage from Figure 4. At a low polymer weight percentage (5 wt%), the hydrogel would not be produced on addition of Fe^{3+}. However, the hydrogel formed with a high polymer weight percentage (15 wt%), would not exhibit the gel-sol transition (Figure S4), which might be related to the higher density of micelles composed of the diblock copolymer P(NIPAM-*co*-NBA)-*b*-P(DMA-*co*-AA).

To further investigate the degradation of hydrogel triggered by UV irradiation, the corresponding measures were conducted on hydrogel samples composed of amphiphilic diblock copolymer with different lengths of the P(NIPAM-*co*-NBA) block, and the corresponding properties of the diblock copolymers were list in Table 1. It could be concluded that both higher Fe^{3+}/COO^- molar ratio and higher polymer weight

percentage were needed for the gelation for the amphiphilic diblock copolymer with longer P(NIPAM-co-NBA) block.

Degradation of hydrogel under EDTA and redox environment

As shown in Scheme 1, there were other two different strategies to trigger the hydrogel to undergo the gel-sol transition except for UV irradiation. Upon addition of EDTA, Fe^{3+} would be removed and the hydrogel would be degraded because of the absence of crosslinking. Reacting with $Na_2S_2O_4$, on one hand, the nitro groups would be reduced to amino groups mildly, followed by 1,4-rearrangement-eliminiation as reported[39-41], leading to the degradation of micelle assembled by amphiphilic diblock copolymer. On the other hand, $Na_2S_2O_4$ would also reduce the Fe^{3+} to Fe^{2+}, leading to the disappearance of the color of Fe^{3+} and a much weaker coordination.

Corresponding rheological measures were undertaken on hydrogels reacting with EDTA and $Na_2S_2O_4$, with varying time intervals, as shown in Figure 5. The degradation of hydrogel triggered by UV irradiation proceeded slowly, which is attributed to the photochemical procedure. The degradation triggered by EDTA proceeded most rapidly, with color fading, owing to the removal of Fe^{3+} by EDTA. The degradation triggered by $Na_2S_2O_4$ proceeded with color disappearing, due to the reduction of Fe^{3+} to Fe^{2+} by $Na_2S_2O_4$.[42] The gel-sol transition underwent in all configurations (triggered by UV irradiation, EDTA or $Na_2S_2O_4$) and all of the values of G', G" and viscosity decreased sharply (~ 90%).

***In vitro* cytotoxicity evaluation before complexation, after complextion and stimuli-triggered degradation**

From the in vitro cytotoxicity evaluation against 4T1 cells, as shown in Figure S6, all of the cell viability in samples before complexation and after degradation triggered by UV, EDTA or $Na_2S_2O_4$ exceeded ~80%, indicating the great biocompatibility and potential of this multi-stimuli responsive supramolecular hydrogel employed for biomedical application.

Conclusions

Multi-stimuli responsive supramolecular hydrogel based on the complexation of Fe^{3+} and amphiphilic diblock copolymer micelles were prepared and characterized. The degradation of hydrogel triggered by EDTA, UV irradiation and $Na_2S_2O_4$ were investigated respectively. It is believed the novel hydrogel integrates degradation mechanism triggered by multiple stimuli would be of great potential for biomedical application.

Acknowledgements

We gratefully acknowledge financial support from the National Natural Science Foundation of China (Grant no. 51273189), National Science and Technology Major Project of the Ministry of Science and Technology of China (2011ZX05010-003).

Notes and references

1. E. A. Appel, J. del Barrio, X. J. Loh and O. A. Scherman, *Chemical Society reviews*, 2012, **41**, 6195-6214.
2. T. Rossow, S. Hackelbusch, P. van Assenbergh and S. Seiffert, *Polymer Chemistry*, 2013, **4**, 2515.
3. T. Vermonden, R. Censi and W. E. Hennink, *Chemical reviews*, 2012, **112**, 2853-2888.
4. J. A. Foster, R. M. Parker, A. M. Belenguer, N. Kishi, S. Sutton, C. Abell and J. R. Nitschke, *Journal of the American Chemical Society*, 2015, **137**, 9722-9729.
5. Z. Sun, F. Lv, L. Cao, L. Liu, Y. Zhang and Z. Lu, *Angewandte Chemie*, 2015, **54**, 7944-7948.
6. L. J. De Cock, S. De Koker, B. G. De Geest, J. Grooten, C. Vervaet, J. P. Remon, G. B. Sukhorukov and M. N. Antipina, *Angewandte Chemie*, 2010, **49**, 6954-6973.
7. W. J. Duncanson, T. Lin, A. R. Abate, S. Seiffert, R. K. Shah and D. A. Weitz, *Lab on a chip*, 2012, **12**, 2135-2145.
8. X. Huang and C. S. Brazel, *Journal of Controlled Release*, 2001, **73**, 121-136.
9. K. E. Uhrich, S. M. Cannizzaro, R. S. Langer and K. M. Shakesheff, *Chemical reviews*, 1999, **99**, 3181-3198.
10. A. Herrmann, *Angewandte Chemie*, 2007, **46**, 5836-5863.
11. Z. Majeed, N. K. Ramli, N. Mansor and Z. Man, *Reviews in Chemical Engineering*, 2015, **31**.
12. P. M. Kharkar, K. L. Kiick and A. M. Kloxin, *Chemical Society reviews*, 2013, **42**, 7335-7372.
13. K. R. Kamath and K. Park, *Advanced Drug Delivery Reviews*, 1993, **11**, 59-84.
14. C. C. Lin and K. S. Anseth, *Pharmaceutical research*, 2009, **26**, 631-643.
15. J. C. Dyke, H. Hu, D. J. Lee, C. C. Ko and W. You, *Journal of materials chemistry. B, Materials for biology and medicine*, 2014, **2**, 7704-7711.
16. J. Hu, G. Zhang and S. Liu, *Chemical Society reviews*, 2012, **41**, 5933-5949.
17. M. A. Stuart, W. T. Huck, J. Genzer, M. Muller, C. Ober, M. Stamm, G. B. Sukhorukov, I. Szleifer, V. V. Tsukruk, M. Urban, F. Winnik, S. Zauscher, I. Luzinov and S. Minko, *Nature materials*, 2010, **9**, 101-113.
18. D. Roy, J. N. Cambre and B. S. Sumerlin, *Progress in Polymer Science*, 2010, **35**, 278-301.
19. C. de Las Heras Alarcon, S. Pennadam and C. Alexander, *Chemical Society reviews*, 2005, **34**, 276-285.
20. Z. Ge, J. Hu, F. Huang and S. Liu, *Angewandte Chemie*, 2009, **48**, 1798-1802.
21. J. Hu, Z. Ge, Y. Zhou, Y. Zhang and S. Liu, *Macromolecules*, 2010, **43**, 5184-5187.
22. C. Zhou, M. A. Hillmyer and T. P. Lodge, *Journal of the American Chemical Society*, 2012, **134**, 10365-10368.
23. I. Koonar, C. Zhou, M. A. Hillmyer, T. P. Lodge and R. A. Siegel, *Langmuir : the ACS journal of surfaces and colloids*, 2012, **28**, 17785-17794.
24. C. Li, N. J. Buurma, I. Haq, C. Turner, S. P. Armes, V. Castelletto, I. W. Hamley and A. L. Lewis, *Langmuir : the ACS journal of surfaces and colloids*, 2005, **21**, 11026-11033.
25. S. Reinicke, J. Schmelz, A. Lapp, M. Karg, T. Hellweg and H. Schmalz, *Soft Matter*, 2009.
26. E. R. Draper, E. G. B. Eden, T. O. McDonald and D. J. Adams, *Nature Chemistry*, 2015, **7**, 848-852.
27. F. Peng, G. Li, X. Liu, S. Wu and Z. Tong, *Journal of the American Chemical Society*, 2008, **130**, 16166-16167.

28. M. He, J. Li, S. Tan, R. Wang and Y. Zhang, *Journal of the American Chemical Society*, 2013, **135**, 18718-18721.
29. N. K. Singh and D. S. Lee, *Journal of controlled release : official journal of the Controlled Release Society*, 2014, **193**, 214-227.
30. N. A. Peppas, R. Duncan, G. E. Wnek, A. S. Hoffman, G. H. Gao, S. W. Kim, D. S. Lee, M. Hadjiargyrou, E. Touitou, D. Ainbinder, R. Mumper, A. Rolland, T. Niidome, V. Labhasetwar, S. Liu, G. Zhou, Y. Huang, Z. Xie, X. Jing, N. Csaba, M. J. Alonso, O. Ali, D. J. Mooney, P. Lönn, S. F. Dowdy, S.-S. Feng, J. Gao, E. S. Lee, K. Na, Y. H. Bae, G. M. Zentner, H. Kim, H. S. Yoo, M. Nakayama, T. Okano, Z.-X. Liao, E.-Y. Chuang, C.-W. Hsiao, H.-W. Sung, H. Cabral, K. Kataoka, P. R. Nair, D. Discher and S. Mitragotri, *Journal of Controlled Release*, 2014, **190**, 29-74.
31. R. Dong, Y. Pang, Y. Su and X. Zhu, *Biomaterials science*, 2015, **3**, 937-954.
32. J. D. Kretlow and A. G. Mikos, *AIChE journal. American Institute of Chemical Engineers*, 2008, **54**, 3048-3067.
33. E. C. Novosel, C. Kleinhans and P. J. Kluger, *Adv Drug Deliv Rev*, 2011, **63**, 300-311.
34. M. W. Tibbitt and K. S. Anseth, *Biotechnology and bioengineering*, 2009, **103**, 655-663.
35. M. K. Gupta, J. R. Martin, T. A. Werfel, T. Shen, J. M. Page and C. L. Duvall, *Journal of the American Chemical Society*, 2014, **136**, 14896-14902.
36. R. Cheng, F. Meng, C. Deng, H. A. Klok and Z. Zhong, *Biomaterials*, 2013, **34**, 3647-3657.
37. L. Ionov and S. Diez, *Journal of the American Chemical Society*, 2009, **131**, 13315-13319.
38. L. Ionov, A. Synytska and S. Diez, *Advanced Functional Materials*, 2008, **18**, 1501-1508.
39. C. A. Blencowe, A. T. Russell, F. Greco, W. Hayes and D. W. Thornthwaite, *Polym. Chem.*, 2011, **2**, 773-790.
40. A. Zheng, D. Shan and B. Wang, *The Journal of Organic Chemistry*, 1999, **64**, 156-161.
41. H. Cho, J. Bae, V. K. Garripelli, J. M. Anderson, H. W. Jun and S. Jo, *Chemical communications*, 2012.
42. H. Minato and M. Iwakawa, *Polymer Journal*, 1974, **6**, 234-237.
43. J. T. Auletta, G. J. LeDonne, K. C. Gronborg, C. D. Ladd, H. Liu, W. W. Clark and T. Y. Meyer, *Macromolecules*, 2015, **48**, 1736-1747.
44. Y. Mitsukami, M. S. Donovan, A. B. Lowe and C. L. McCormick, *Macromolecules*, 2001, **34**, 2248-2256.
45. Q. Li, Y. Bao, H. Wang, F. Du, Q. Li, B. Jin and R. Bai, *Polymer Chemistry*, 2013, **4**, 2891.
46. T. Spychaj and B. Schmidt, *Macromolecular Symposia*, 2000, **152**, 173-189.
47. H. H. Winter, *Journal of Rheology*, 1986, **30**, 367.
48. V. S. Rudraraju and C. M. Wyandt, *International journal of pharmaceutics*, 2005, **292**, 63-73.
49. Z. Wei, J. He, T. Liang, H. Oh, J. Athas, Z. Tong, C. Wang and Z. Nie, *Polymer Chemistry*, 2013, **4**, 4601.
50. U. Gulyuz and O. Okay, *Soft Matter*, 2013, **9**, 10287.
51. Z. Wei, J. H. Yang, J. Zhou, F. Xu, M. Zrinyi, P. H. Dussault, Y. Osada and Y. M. Chen, *Chemical Society reviews*, 2014, **43**, 8114-8131.
52. Y. Zhang, L. Tao, S. Li and Y. Wei, *Biomacromolecules*, 2011, **12**, 2894-2901.
53. M. Ehrbar, R. Schoenmakers, E. H. Christen, M. Fussenegger and W. Weber, *Nature materials*, 2008, **7**, 800-804.

Abstract

The stimuli-triggered degradable hydrogels have found broad applications in controlled release of drugs, fragrances, flavourings and fertilizers. Recently, multi-stimuli responsive micelle-based hydrogels has become focus, since they could respond to a combination of external stimulus. Herein, a multi-stimuli responsive supramolecular hydrogel with great potential to biomedical application was prepared, which composed of the micelle-forming diblock copolymer poly[(N-isopropylacrylamide-*co*-2-nitrobenzyl acrylate)-*block*-(N,N-dimethylacrylamide-*co*-acrylic acid)] (P(NIPAM-*co*-NBA)-*b*-P(DMA-*co*-AA)), and physically cross-linked by supramolecular complexation between AA groups and ferric ions (Fe^{3+}), exhibiting gel-sol transition by UV irradiation, multidentate ligands (EDTA) and redox agent ($Na_2S_2O_4$).